João Rios Crespo
Licenciado em Engenharia de Micro e Nanotecnologias

Electrochemical-SERS analysis of R6G using a microcontroller based Portable Potentiostat

Dissertação para obtenção do Grau de Mestre em
Engenharia Micro e Nanotecnologias

Orientador: Dr Tanya Hutter, Department of Chemistry, University of Cambridge

Co-orientador: Prof. Doutor Hugo Manuel Brito Águas, Faculdade de Ciências e Tecnologia da Universidade Nova de Lisboa

Júri:

Presidente: Prof. Doutor Luís Pereira

Arguentes: Prof. Doutor Rui Igreja

Vogais: Prof. Doutor Hugo Águas

FACULDADE DE CIÊNCIAS E TECNOLOGIA
UNIVERSIDADE NOVA DE LISBOA

November, 2017

Electrochemical-SERS analysis of R6G using a microcontroller based Portable Potentiostat

.

Acknowledgements

In the end of this long and important stage of my life, I would like to thank to all of those who made this possible, the ones who help me and made this moment possible. That being said, I start by thanking a lot the Faculty of Science and Technology from Nova University of Lisbon, specially to Department of Materials Science for having me throughout all this years in such a good way. All of this was only possible because Prof. Dr. Rodrigo Martins and Prof. Dr. Elvira Fortunato created Engineering of Micro and Nanotechnology course which gave me the tools, the critical thinking, and good labs procedures that an engineer must have.

I would like to thank Dr Tanya Hutter and Dr Stephen Elliott for accepting me at the Department of Chemistry at University of Cambridge and providing me all the tools and orientation to make this thesis possible. I also would like to thank Vicky for the Raman training, Andrew for all the lab procedure tips, Farah for her friendly and joyful presence and, without excluding anyone, all the Stephen Elliott's group for having me in such a kind way and for our inspiring discussions.

Finally, I would like to thank my family, specially my father, for all the unconditional support which was fundamental, making me say that I am a very lucky person.

Resumo

Os primeiros espectros de Raman aumentados pela superfície foram obtidos a partir de uma célula eletroquímica, o que levou à descoberta do efeito SERS (Surface-Enhanced Raman Spectroscopy) em meados da década de 1970. Até à data, muitos artigos foram publicados em vários aspetos do SERS a partir de sistemas eletroquímicos. O SERS consiste em uma técnica muito sensível para a deteção de analitos em concentrações muito baixas. Além disso, SERS pode fornecer informações sobre como os analitos interagem com a superfície metálica, tornando-se uma técnica muito útil para engenharia e investigação de superfícies.

A fim de explorar plenamente essa interação metal-analito, SERS tem sido utilizado em um ambiente eletroquímico. Assim, nesta designada técnica Electrochemical-SERS (EC-SERS) existem duas propriedades distintamente diferentes de campos elétricos, um campo eletromagnético e um campo eletroquímico estático, coexistindo na interface do eletrólito, contendo o analito alvo, e o elétrodo metálico nanoestruturado. Para aplicar o potencial desejado no elétrodo de trabalho nanoestruturado, um dispositivo portátil designado de potenciostato baseado utilizando um microcontrolador foi projetado para ser instalado no microscópio Raman juntamente com uma célula eletroquímica que pode conter o eletrólito e os respetivos elétrodos para executar simultaneamente medidas SERS.

Grandes esforços têm sido feitos para entender compreensivamente os espectros SERS e EC-SERS com base nos mecanismos de aumento físico e químico para fornecer informações significativas para revelar os mecanismos de adsorção e reação eletroquímica.

Finalmente, utilizou-se Rhodamine-6G como analito alvo para medidas EC-SERS com o objetivo de fornecer uma nova visão dos mecanismos de transferência de carga relatados em cálculos teóricos que são difíceis de detetar experimentalmente usando energias de excitação mais elevadas devido à forte fluorescência.

Palavras-chave: Rhodamine 6G; Espectroscopia de Raman reforçada com superfície eletroquímica (EC-SERS); potenciador

Abstract

The first Surface-Enhanced Raman Spectroscopy (SERS) spectra were obtained from an electrochemical cell, which led to the discovery of the SERS effect in mid-1970s. Up to date, a lot of papers have been published on various aspects of SERS from electrochemical systems. SERS consists in a very sensitive technique for detection of analytes at very low concentrations. Furthermore, SERS can give information of how the analytes interacts with the metal surface, becoming a very useful technique for surface engineering and research.

To fully explore this metal-analyte interaction SERS has been perform in an electrochemical environment. Thus, in this Electrochemical-SERS (EC-SERS) technique there are two distinctively different properties of electric fields, an electromagnetic field and a static electrochemical field, co-existing in electrochemical systems in the interface of the electrolyte, containing the target analyte, and the nanostructured metal electrode. To apply the desired potential at the nanostructured working electrode, a microcontroller based portable potentiostat device was design and fabricated to fit in the Raman microscope along with an electrochemical cell that can hold the electrolyte and the respective electrodes to perform simultaneously SERS measurements.

Great efforts have been done to comprehensively understand SERS and EC-SERS spectra based on the chemical and physical enhancement mechanisms to provide meaningful information for revealing the mechanisms of electrochemical adsorption and reaction.

Finally, Rhodamine-6G was used as target analyte for EC-SERS measurements with the objective of providing a new insight of the charge transfer mechanisms reported in theoretical calculations which are hard to detect experimentally using higher excitation energies due to the strong fluorescence yield.

Keywords: Rhodamine 6G; Electrochemical-Surface enhanced Raman spectroscopy (EC-SERS); potentiostat

Contents

Index of tables

Chapter 2 - Design and fabrication of a Portable Potentiostat

Chapter 5 - Results and discussion

Index of figures

Chapter 5 - Results and discussion

Abbreviation index

RE – Reference Electrode

CE – Counter Electrode

WE – Working Electrode

Au – Gold

Ag – Silver

Ag/AgCl – Silver/Silver Chloride saturated electrode

Pt – Platinum

TIA - Transimpedance Amplifier

VF – Voltage Follower

CA – Control Amplifier

SERS – Surface Enhanced Raman Spectroscopy

EC-SERS – Electrochemical SERS

PWM – Pulse Width Modulation

Op-amp – Operational Amplifier

Vpp – Peak to Peak Voltage

DA – Differential amplifier

µA – Micro amperes

Ex. λ – Excitation wavelength

CV – Cyclic Voltammograms

EF – enhancement facto

1 Introduction

1.1 Surface-Enhanced Raman Microscopy

Raman spectroscopy, as a vibrational spectroscopy can give information about surface bonding, conformation and orientation of the targets molecules, making it one of the most promising methods for spectroscopic studies of surface-molecule interactions. The big disadvantage is its low detection sensitivity making this technique almost impractical. However, Surface-enhanced Raman Spectroscopy can improve the sensitivity by several orders of magnitude for roughened surfaces of noble (e.g. Au, Ag and Cu) and many transition (e.g. Pt, Ru, Rh, Pd, Fe, Co and Ni) metals. [1]

The enhancement of the Raman signal arises from the combination of the Electromagnetic Enhancement Chemical enhancement mechanisms. The electromagnetic enhancement (EM) is due to the interaction of an electromagnetic wave with a metal surface. The electromagnetic wave, with a specific energy, excites resonantly the delocalized conduction electrons in a metal (plasmon), resulting in an amplification of the electromagnetic fields near the surface.[2] When the valence electrons of the metal nanostructure are in a collective oscillation with the frequency of the incident light, occurs the LSPR. The Chemical enhancement mechanism is generated by the direct interaction of adsorbed molecules with the metal surface, which results in a charge transfer, leading to changes in the polarizability and vibrational modes, resulting a change of the Raman scattering cross-section of the molecule that will lead to enhancements in the range of one to three order of magnitude for Raman scattering, significantly smaller than EM.[3]

1.2 Electrochemical Surface-enhanced Raman Spectroscopy (EC-SERS)

The EC-SERS system consists of introducing a conductive and nanostructured electrode in an electrochemical cell as the working electrode which is then put in contact with an electrolyte solution containing the target molecule to be studied. Like SERS, EC-SERS can be divided in two different purposes: characterization or identification. For characterization purpose one should have more comprehensive and understanding of the SERS regarding the enhancement mechanism and surface selection rules to understand how the analyte interacts with the SERS substrate. For identification purpose, the objective is to detect the target species in terms of sensitivity and selectivity.

In the EC-SERS system both electromagnetic and chemical enhancement mechanisms can be influenced by the changing of the potential applied in the electrode, i.e., one can change the fermi level of the Metal and the dielectric constant of the interfacial electrolyte and this will lead to a change in the interface structure properties. [4]

1.3 Electrochemical double layer in EC-SERS system

In the Figure 1 is depicted the SERS process in the electrochemical double layer region. A laser light beam illuminates the nanostructured electrode surface from the top and excites the SERS process. In this region, there are two types of electric fields coexisting: an alternating electromagnetic (EM) field and a static electrochemical (EC) field. The EC field is established mainly over the compact layer with about a few nm of thickness due to the big potential drop over this layer and decreasing its intensity over the diffuse layer.

This EC field influences the interaction between the electrode surface and the molecules present in the electrolyte and by changing the double layer structure it may in turn change the plasmon generated by the laser. Also, by tuning the potential of the electrode the density and the polarity of charges of the surface can be changed. When the potential is more positive than the point of zero charge (PZC) the surface will be more positively charged and the Water molecules will interact via negatively charged O, likewise other anionic species in the electrolyte may also interact. As shown in the (Figure 1a) pyridine molecules, as example, can repel water molecules and interact the surface via both delocalized π-orbital or the lone-pair of the Nitrogen atom in a tilted configuration. When the electrode surface potential is switched to more negative than the PZC, the reverse happens. The water molecules interact via the Hydrogen atoms and the pyridine may interact via the lone-pair of the Nitrogen atom in a vertical configuration (Figure 1b). With more negative electrode potentials the analyte/electrode surface interaction becomes weaker and might change from chemisorbed to physisorbed with pyridine even desorbing from the surface.[4]

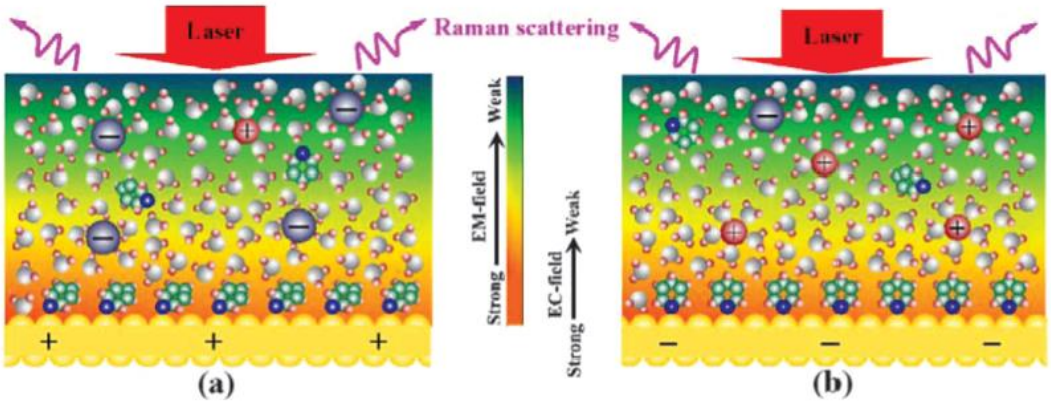

Figure 1 – Schematic Diagrams of the Electrochemical interfaces with the coexistence of electrochemical field induced by the Laser and electric field at the electrode potentials. (a) positive or (b) negative to the potential of zero charge. Adapted from [5].

1.4 Electrode Materials

The optical properties of a material are a lot related to its electronic structure. The coinage Metals are the most SERS-active substrates which have this optical property due to the free electrons, that characterize the metal bond, which supports the Surface plasmon resonance (SPR). But the SPR effect is severely quenched for Copper (Co) and Gold (Au) due to the d-sp electronic transitions when excitation energies are higher than 2.2 eV whereas the interband electronic transition of Silver occurs at energies higher than 3.8 eV making it more useful for smaller excitation wavelengths.[6]

If a strong chemical bond is formed, it will change the electronics structure of the adsorbate as well as the electronic structure of the surface. This may cause a change in the SPR energy, changing this way the electromagnetic field at the metal surface.[7] Also, if the electronic structure of the adsorbate is changed it may cause different enhancements for different vibrational modes.[8]

1.5 The electrochemically influenced SERS enhancement

As aforementioned, by changing the applied potential one can change the charge density and polarity of the electrode surface resulting in a shift of the SPR wavelength. [9] [10]

The SERS intensity dependency of the potential and metal type observed in many EC-SERS system gives strong evidence that the Chemical enhancement is cooperative with Electromagnetic enhancement. [5] [4]

In the Figure 2 is illustrated the photon driven charge transfer (CT) mechanism with HOMO and LUMO, denoted as the highest occupied molecular orbital and the lowest unoccupied molecular orbital, respectively, of the adsorbed molecules along with the energy of the Fermi level at the electrode when the Potential of Zero Charge is applied (V_0). As can be seen in the figure at the potential of V_0, it is insufficient to produce the photon-driven CT state on the surface with the excitation energy of hv. Thus, the SERS intensity in this potential region is mainly explained by the bonding mechanism. When the potential applied is changed to V_1, it will increase of the Fermi level of the Metal and the excitation energy matches the required CT energy to excite the vibrational modes leading to an enhancement of the SERS intensity in a resonance-like Raman scattering. [5]

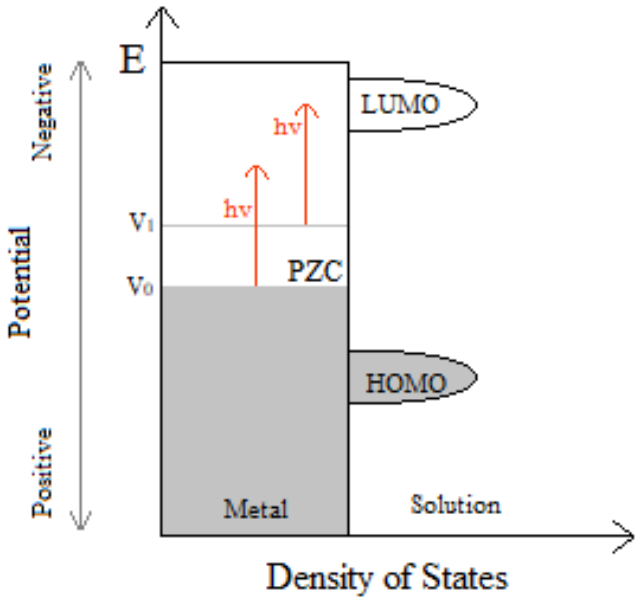

Figure 2 – Schematic energy (density of states) of the photon-driven Charge transfer mechanisms from a Metal electrode to an adsorbed molecule in the EC-SERS system

It is clearly displayed that by changing the surface energy with the applied potential one can excite different vibrational states of the adsorbate due to the interaction of the metal adsorbate mechanism. Besides the characterization purpose, if the right potential is chosen at which the adsorbed molecule shows the highest signal intensity, one will be able to improve the detection sensitivity.

1.6 Applications of EC-SERS

From the above description of EC-SERS, three applications can be attributed: (I)the detailed investigation and characterization of molecule substrate interaction under different electrochemical potentials, (II) improve detection sensitivity by selecting the right potential (III) and study how different target molecules interact with each other when present in the same electrolyte.

1.7 SERS Analyte

In the present work, the SERS analyte used was Rhodamine 6G (R6G). Due to its high Raman cross-section, this compound is commonly used as an analyte to evaluate SERS activity in the substrates.

Rhodamine 6G has been study using DFT theoretical calculations [11][12] and most of the SERS vibrational peaks measured were successfully assign.[13] Also, SERRS and off-resonance SERS study have been performed showing the possibility of a charge transfer mechanism due to the interaction of R6G and the substrate.[13]

Its structure, shown in the Figure 3 ,consists of a xanthene ring substituted by two methyl groups, two ethylamino groups, and a carboxyphenyl group.

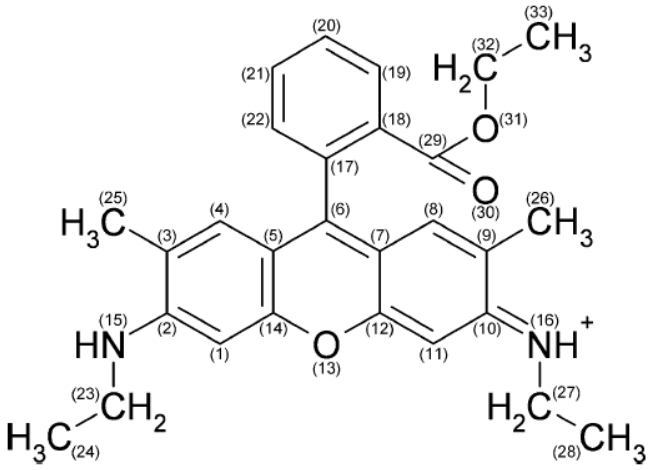

Figure 3- Structure of rhodamine 6G and atomic numbering.

In present work, the objective is to perform a potential dependent SERS spectra study of Rhodamine 6G to identify the presence of any charge transfer state using Silver and Gold SERS substrates. The Rhodamine 6G used was purchased from Sigma Aldrich without any further purification.

1.8 Potentiostat

The potentiostat is an electronic circuit commonly used in electrochemistry. To study the electrochemical events taking place at one specific electrode, the Working electrode(WE), a three-electrode potentiostat with a separate Reference (RE) and Counter (CE) electrode allows the potential and the current at the WE to be measured with little or no “interference” or “contribution” from the other electrodes.

So, the potentiostat injects a current into the cell through the counter electrode (CE) and measures the current flowing through WE, where the electrochemical reaction is taking place. A third electrode, the reference electrode (RE), is also introduced to the cell with the function of measuring the potential applied in the cell. To do it with minimal interference it should have a constant electrochemical potential and no current must flow through it. The most common lab Reference Electrodes are the saturated calomel electrode (SCE) and the silver/silver chloride (Ag/AgCl) electrodes.

A simple potentiostat circuit is shown in the Figure 4, the Control Amplifier (CA), is a servo amplifier. It compares the measured Cell voltage with the desire voltage and drives current into the cell to force the voltages to be the same in an inverting configuration to provide the negative feedback.

The Voltage follower (VF), sometimes also referred as Electrometer, measures the voltage of the RE and the output signal is introduced in the feedback loop and it is the signal that is measured whenever the cell voltage is needed.

An ideal VF has zero input current and an infinite input impedance. Current flow through the reference electrode can change its potential. In practice, all modern VF amplifiers have input currents close enough to zero that this effect can usually be ignored.

The transimpedance amplifier (TIA), converts the measured current in the WE into a voltage through the resistance R_f. The cell current in some experiments don't change much. In other experiments, when electrochemical reactions occur, the current can often vary by as much as orders of magnitude, so it is of interest to use different values of the R_f to allow the measurement of widely varying currents. Other important feature of this amplifier is forcing ground voltage in the WE by connecting the non-inverting input to ground. This way the voltages values are measured relative to grounded WE.

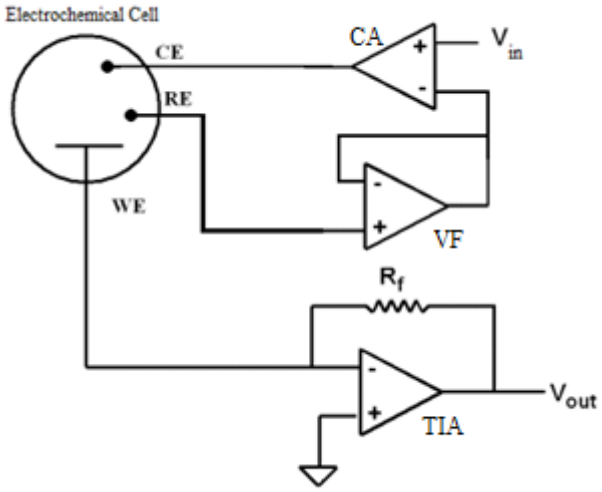

Figure 4 – Basic potentiostat circuit

The Signal (V_{in}) is a computer-controlled voltage source. It is generally an output of a Digital-to-Analog (D/A) converter that converts a digital signal into an analog signal.

Different types of electrochemical experiments depend mostly on the type of the signal applied to the cell. If the signal output is a linear voltage ramp is called Linear Sweep voltammetry, if the signal is a linear voltage ramp that returns to the initial value, (triangular shape), it is called cyclic voltammetry. Other very often used electrochemical experiment is called chronoamperometry where a constant voltage signal is applied and the current is measured over time.

2 Design and fabrication of a Portable Potentiostat

The primary objective was to design and develop a microcontroller-based portable potentiostat. Numerous commercial instruments that perform such analysis are available, however, their size inhibit their application due to small space left inside the Raman microscope where the potentiostat must fit in to perform EC-SERS measurements.

Also, commercial potentiostats are design to be a user-friendly equipment, but in fact, they end up preventing the full usage of the equipment capabilities and true understanding of the collected data. And to perform EC-SERS, there was a need to have an potentiostat where the applied voltage is easily controlled by the user to combine with Raman measurements during the Voltage scan.

In this scope, Arduino microcontroller boards based on the ATMega microcontroller family stand out because of their outstanding capabilities, affordable price and portability. Also, this boards have digital outputs which go up to 5V and most of Electrochemical experiments are performed within the range of ± 2 V which make this boards capable of producing the required output voltage range with the help of a voltage shifter circuit.

On this note, it is presented the design and fabrication of a simple, cheap, and customizable Arduino based potentiostat that relies only on open software programs and few electronic components capable of performing electrochemical measurements.

2.1 Potentiostat Circuit design

The Potentiostat Circuit developed, present in the Figure 5, was inspired by the potentiostat circuit proposed by [14].

The major potentiostat circuit differences are the use of a single op-amp U1 for signal supply and shifting, with the aim of reducing the total number of op-amps used. Also, instead of using a ladder circuit to supply the signal from the I/O microcontroller ports to the potentiostat circuit a simple RC filter was introduced. In the present work, an Arduino Uno board was used which is equipped with a microcontroller ATmega328.

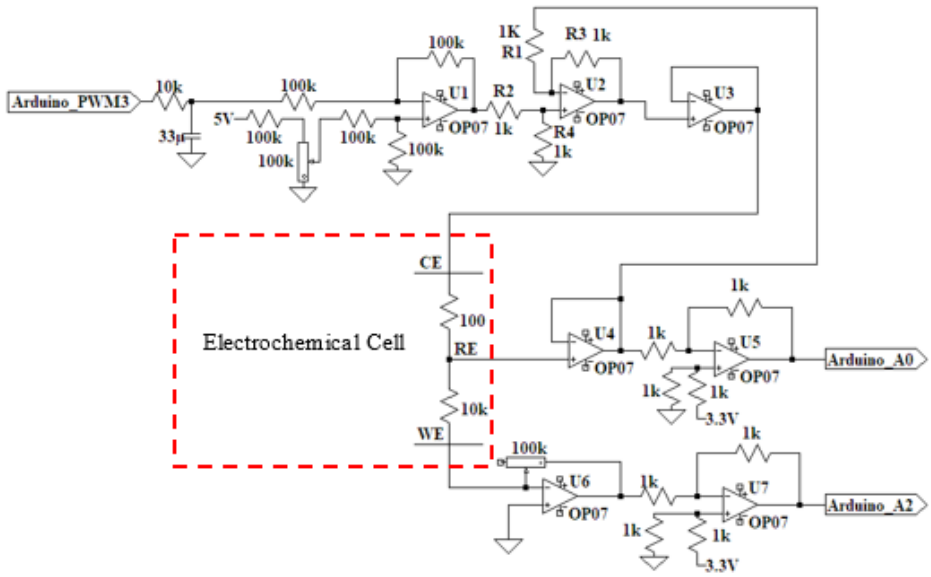

Figure 5 – Portable Potentiostat analog circuit with the Electrochemical Cell highlighted.

2.2 Operation of the Potentiostat

2.2.1 RC Low Pass filter

Pulse Width Modulation, or PWM, is a technique for getting analog results with digital means. Digital control is used to create a square wave, a signal switched between on and off. This on-off pattern can simulate voltages in between full on (5 Volts) and off (0 Volts) by changing the portion of the time the signal spends on versus the time that the signal spends off. However, in electrochemical measurements it is desire to have a DC like signal where the high frequencies are removed. To do this a RC filter was introduced which is compose by a resistance and a capacitor, this is shown in the Figure 6.

The Sizing of the RC filter circuit was made to have a Peak-to-peak ripple voltage smaller than a tenth of the minimum PWM resolution which is $\frac{5\,V}{2^8-1} \approx 20mV$.

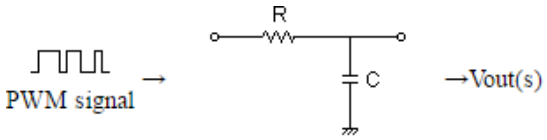

Figure 6 -Basic RC Low Pass Filter Circuit

2.2.2 Op-amp U1

The Op-amp U1 is a Differential Amplifier (DA) and it has the function of driving the input signal from the Arduino PWM output and add offset voltage value, from the voltage divider composed by the 100K resistors and the 100k potentiometer in the non-inverting input, to shift the applied voltage to the cell in the desired range. The potentiometer is used so the user can tune manually the applied voltage range.

2.2.3 Op-amp U2

The Op-amp U2, as aforementioned, has the roll of the Control Amplifier. It compares the measured Cell voltage with the desire voltage and drives current into the cell to force the voltages to be the same in an inverting configuration to provide the negative feedback. This can be described by the following equations:

At the summing point,

$$V^- = V^+ \quad (1)$$

$$V^- = V^+ = V_{in}\left(\frac{R_4}{R_2 + R_4}\right) \quad (2)$$

If $V_{in} = 0$,

$$V'_{out} = -V_{RE}\frac{R_3}{R_1} \quad (3)$$

If $V_{RE} = 0$,

$$V''_{out} = V_{in}\left(\frac{R_4}{R_2 + R_4}\right)\left(\frac{R_1 + R_3}{R_1}\right) \quad (4)$$

Using the superposition theorem,

$$V_{out} = V'_{out} + V''_{out} \quad (5)$$

If all the resistors are of the same value, that is R1 = R2 = R3 = R4, then,

$$V_{out} = V_{in} - V_{RE} \qquad (6)$$

the op-amp U2 becomes a unity gain differential amplifier.

2.2.4 Op amp U3

The Op-amp U3 is a voltage Follower that isolates the input from the output to prevent loading of the input signal. The voltage output from op-amp U3 was connected to the CE.

2.2.5 Op amp U4

The Op-amp U4 is a voltage follower and it has the function described previously for the Electrometer.

2.2.6 Op amp U5 and U7

Both the Op amp U5 and U7 have the function of voltage shifters and they sum 3.3 V from the Arduino to the output signals of the potentiostat, i.e. the voltage and the current measured. They are used because Arduino only can read voltage values from 0 to 5000 mV.

Thus, one can determine the maximum applied voltage ranges that can be read by the Portable Potentiostat which is from -3300 mV to +1700 mV. Even though is it not centered in 0 V it still matches most of the electrochemical applications ranges.

2.2.7 Op amp U6

The Op-amp U6 is a transimpedance amplifier and it has the function described previously for the TIA. The 10-100 kΩ gain potentiometer was used to read currents in the ranges from µA to mA where most of the electrochemical reactions take place.

2.3 Simulation

To simulate the circuit shown in the Figure 5 the LTspice programme was used. A sine wave source was introduced in the circuit input called Arduino_PWM to represent a triangular shape function performed in cyclic voltammetry. All the op amps used were OP07, and they were supplied with +9V and -9V in the rails. The 10 seconds transient response of the circuit is shown in the Figure 7. The input function is represented in a green positive sine wave with an amplitude of 2 V_{pp}.

To shift the input function (shown in green) to be centered in 0 V, 1 V was added by the voltage divider made of the 100 kΩ resistors and the 100 kΩ potentiometer connected in the positive input of the op amp U1. The generated wave applied to the cell through the CE (V(ce), shown in blue) is inverted comparing to the input signal due to the inversion of the negative input signal caused by the Differential Amplifier (U1).

The current sensed by the WE is converted into an inverted voltage value through the TIA (op amp U6), then the signal is again inverted and 3.3 V are added by the Differential Amplifier U7, which sends the signal to the Arduino Analog input (A2), the resulting wave is shown in purple and it can be observed that is in phase with the input signal in blue.

Finally, the voltage sensed by the RE is sent by the VF U4, to the Differential Amplifier U5, which converts it into an inverted value and add 3.3 V to be written in the Arduino Analog input (A0), the resulting wave is shown in red and it can be observed that is in 180° out of phase with the input signal in blue, as expected.

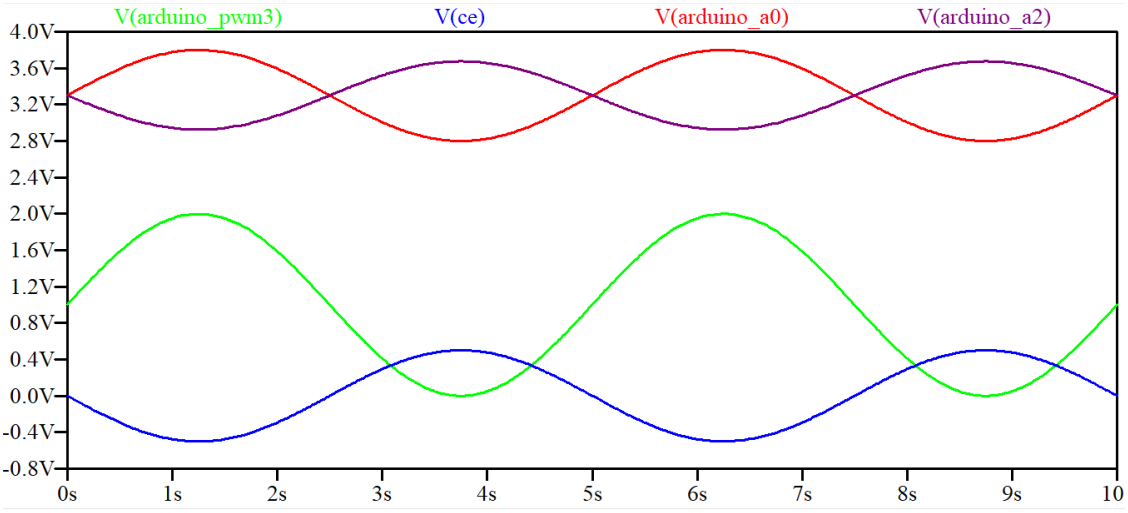

Figure 7 – Waveforms generated in LTspice of the portable potentiostat analog circuit.

2.4 Arduino Software

To Perform Cyclic voltammetry, a triangular-shaped output voltage curve must be applied to the Counter electrode.

To perform such output voltage scan, a step function was implemented using two *for* loops, one that increments (forward direction of the cycle) and other that decrements (reverse direction of the cycle) the value in the *analogwrite()* function in each cycle, as shown in the Figure 8. The *analogwrite()* function will increase and decrease, respectively, the duty cycle of the PWM output pin. The signal is then filtered and an offset is added by the potentiostat circuit before it is applied to the Counter Electrode. The result output function is shown in the Figure 9.

By changing the *maxvoltage* value one can define the range of the applied voltage.

```
//Cyclic Voltametry function
void loop() {
  int maxvoltage = 120;//voltage range
  int voltage_scan = 1;
  delay(2000);//waits to stabilize the voltage values
  for (int i=0; i <maxvoltage; i=i+voltage_scan){
      analogWrite(3, i);
      findAverage();
  }
  for (int i=maxvoltage; i>0; i=i-voltage_scan){
      analogWrite(3,i);
      findAverage();
  }
  delay(2000);//waits to stabilize the voltage values
  analogWrite(2,LOW);
  Serial.flush();
 while(1);//leaves arduino in a invisible loop
 }
```

Figure 8- Cyclic voltammetry function code.

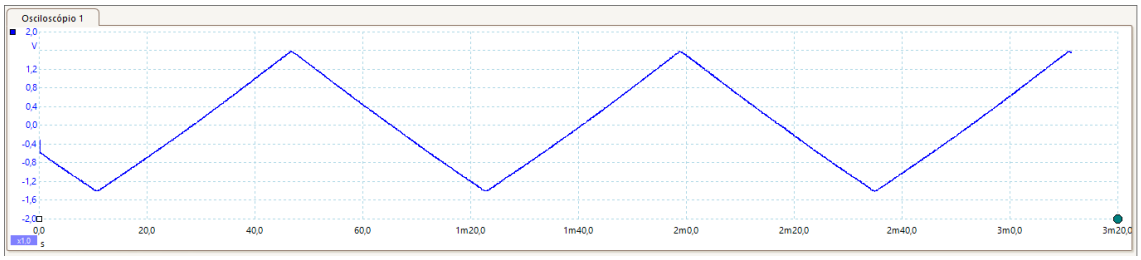

Figure 9 – Output voltage applied to the Counter Electrode when cyclic voltammetry function was performed, measured with an oscilloscope (picoscope 2000 series).

The *findAverage()* function, shown in the Figure 10, reads 9 values in each step and calculates the average voltage and the average current values. The 3.3V are subtracted to the current averaged value to remove the offset imposed by the voltage shifter op amp U7.

Due to the inversion of the average voltage signal read imposed the op amp U5 the value is then multiplied by -1 and 3.3V are added to obtain the real voltage value.

In fact, the calculated current value by the Arduino is a voltage value which then needs to be divided by the resistance of the TIA gain potentiometer to obtain the real current measured in the working electrode.

By changing the *steptime* constant one can change the duration of each step and this means to choose the scan rate of the cyclic voltammogram.

```
void findAverage(){
  float voltage_ave=0;
  float current_ave =0;
  int steptime = 85; // Step time in ms
  int y = 0;
  for(y=0;y<8;y++){
      delay(steptime/8);
      float voltage = analogRead(0);
      float current = analogRead(2);
      voltage_ave = (voltage_ave + voltage)/2;
      current_ave = (current_ave + current)/2;
  }
  voltage_ave = (voltage_ave*5/1023)*-1+3.3;
  current_ave = (current_ave*5/1023)-3.3;
  Serial.print(voltage_ave);
  Serial.print(" ");
  Serial.println(current_ave);
}
```

Figure 10 – FindAverage () function code.

To perform EC-SERS measurements it is useful to have a function where the user can easily measure a Raman spectrum between each step of the potential scan. To achieve the best control of the experiment where the potential scan and the Raman measure were coordinated, a constant potential over time function was built, as shown in the Figure 11.

This function applies an initial constant potential and then the user can change the applied potential by rotating the potentiometer connected to the U1 introducing an offset. Also, this function prints the time of the experiment for EC-SERS measurements over time.

```
//constant potential over time function
void loop() {
   for(int i=0;i<1200;i++){
       analogWrite(3,150);//applied potential value
       float times = millis()/100; //prints time since program started
       Serial.print(times);
       Serial.print(" ");
       findAverage();
       delay(250);// wait a moment to not send massive amounts of data
  }
  analogWrite(2,LOW);
  Serial.flush();
  while(1);//leaves arduino in a invisible loop
 }
```

Figure 11 - Constant potential over time function

2.5 Processing Software

All the values measured by the Arduino Board when cyclic voltammetry is performed are sent to the Serial port which can then be seen in the serial monitor. However, is it of interest to save de values in a text file for further analysis. Also, it is very handy to see the cyclic voltammogram in real time for the user to have a better perception of what is happing when the electrochemical experiment is running.

Processing is an open source programming software sketchbook which has a Serial library that can read serial values from a USB port, it also has the Print Writer library that can create or open text files and print values in it. Also has the function that creates windows for drawing geometric shapes on it.

By this means, *Processing* software was used. The function developed draws a graph where the x axis is the voltage and the y axis is the current. Then it reads in cycle the Serial value from a specified USB port and converts it from a string to a float number. Then this float number is sized to the axis using the map function and finally it is printed on a graph in the drawing window and it is saved in a text file. This function works until the last value of the Serial port is read. The function code is in Attachments.

2.6 Potentiostat circuit on a Breadboard

The potentiostat circuit was first mounted and tested on a breadboard, as shown in the Figure 12.

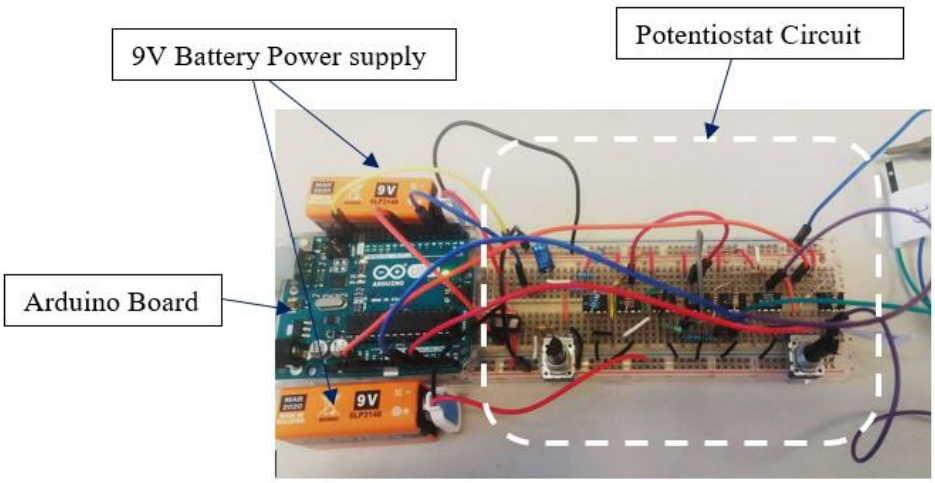

Figure 12 - Portable Potentiostat circuit mounted on the bread board with highlighted the main parts.

2.7 Transfer to an Arduino shield Board

To make the potentiostat more compact and robust the circuit was transferred to a Board with cooper strips printed on it. The components were soldered on the top side and the connections were made by soldering wires on the back side of the Board. This can be visualized in the Figure 13.

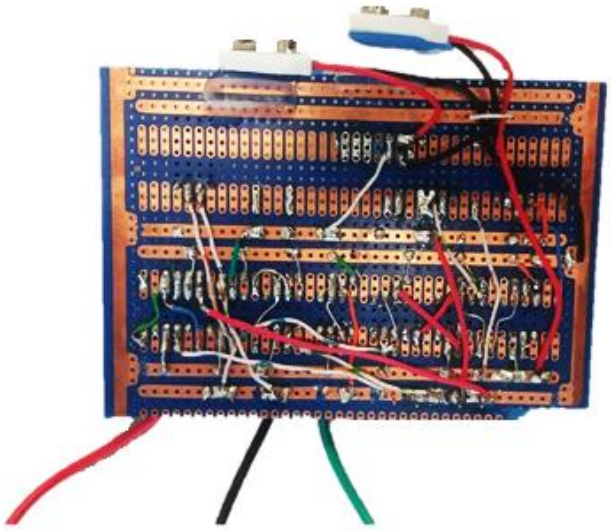

Figure 13 -Back side of the Potentiostat board showing the connections of wires and solder.

The Potentiostat board fits on the top of the Arduino and the connections were made using soldered pins, as shown in the Figure 14.

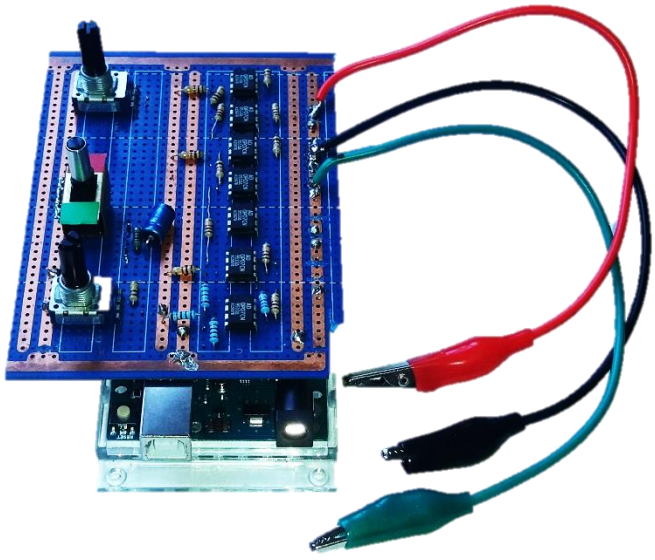

Figure 14 – Portable Potentiostat Arduino Shield Board-

2.8 Testing the Portable Potentiostat

To evaluate the fabricated potentiostat and to verify if it was working as expected 10 a 20 kΩ resistors were used. The well-known response of a resistor also makes it a good component to evaluate the performance since when the voltage is swapped the measured current responds linearly with a slope value of (1/R). The resistors were connected between the working electrode and reference electrode

(simulating the cell resistance) and a small resistor (100 Ω) was connected between the reference and the counter electrode to have the control of the potential applied. A CV of the resistors was recorded it is shown in Figure 15.

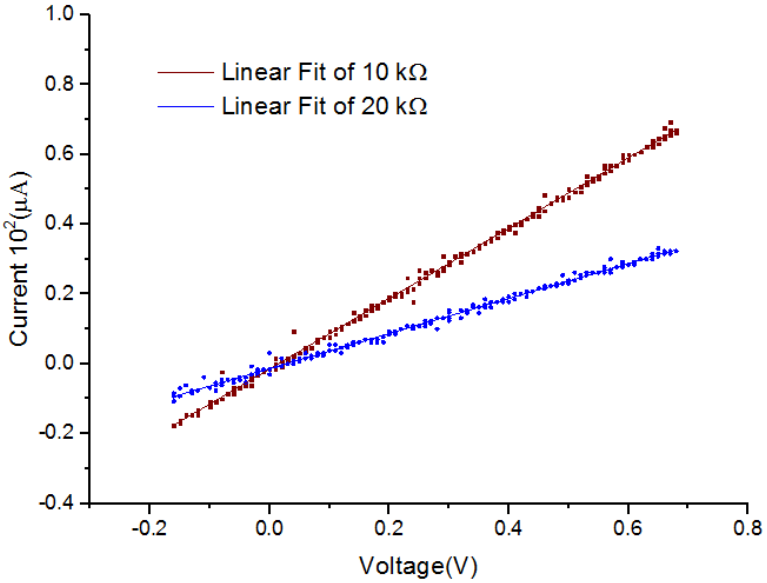

Figure 15 - IV curve of the 10 and 20 kΩ resistors.

Table 1 - Values obtained of the linear fits in the Figure 15.

	Slope (10^{-4} Ω^{-1})	Slope $\sigma_{\bar{x}}$	R^2
10 kΩ	1.0078	0.00339	0.997
20 kΩ	0.5013	0.00248	0.995

From the Table 1, the resistance values were calculated to be 9.992 ± 0,033 kΩ and 19.948 ± 0,098 kΩ for 10 and 20 kΩ, respectively. These values are in good agreement with 10% tolerance of the resistor used

2.8.1 Current resolution

The microcontroller's 10-bit ADC reads this voltage at the following resolution:

$$Resolution = \frac{5000\ mV}{2^{10}} = 4.8\ mV \approx 5mV \quad (7)$$

Also the current is measured through the transimpedance amplifier and the resistance R_f .The voltage drop across R_f was connected to one of the microcontroller's ADC channels. The current was eventually determined by the implementation of Ohm's law in the control software program based on the measured voltage and the value of Rf.

The current measurement resolution depends on the voltage read resolution of the microcontroller's ADC (5 mV calculated above), and the value of Rf . The calculated minimum current detectable by the potentiostat circuit was thus determined using Ohm's law as follows:

$$\text{Resolution} = \frac{5\ mV}{100\ K\Omega} = 0.05\ uA \quad (8)$$

To assess experimentally the current resolution of the Portable Potentiostat, it was measured the maximum cell resistance that the potentiostat can read without introducing significant error. The gain

potentiometer in the TIA was rotate to the maximum value and the IV curves of 100, 200 and 400 kΩ resistor were measured, represented in the Figure 16.

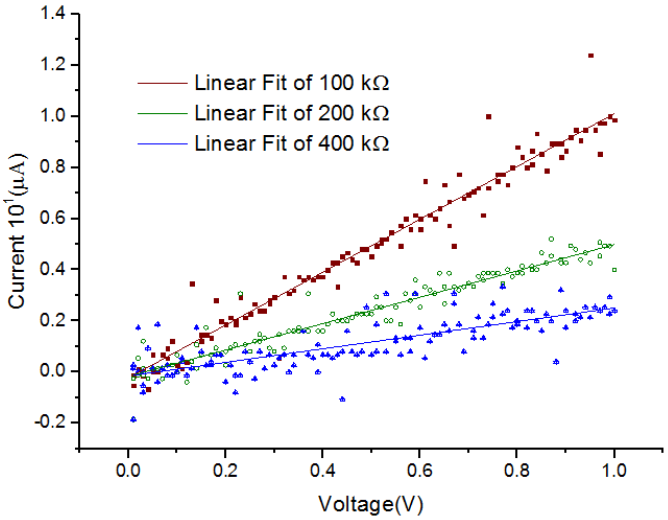

Figure 16 – IV curves of 100 KΩ, 200 KΩ and 400 KΩ resistors.

Table 2- Values obtained of the linear fits in the Figure 16.

	Slope (10^{-5} Ω^{-1})	Slope $\sigma_{\bar{x}}$	R^2
100 kΩ	1.0343	0.01943	0.959
200 kΩ	0.5158	0.01339	0.925
400 kΩ	0.2662	0.02006	0.595

In the Table 2, it can be observed that the higher the resistance the lower the R^2, and so the that 200 KΩ resistor was used as the maximum value that can be measured. Using the 200 KΩ resistor, the current was measured over time under different applied potentials, see Figure 17, and as can be observed the current values can be discriminated from each other although the signals show noise.

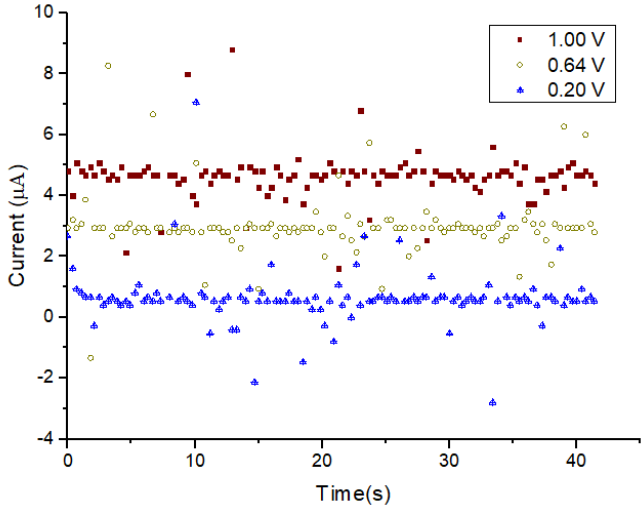

Figure 17 – Current measured over time using a 200 KΩ resistor for different applied voltages.

However, the calculated current resolution values where determined to be 0.05 μA, experimentally it was determined to be in the range of 1 μA due to the noise.

3 Electrochemical performance

3.1 Design of an Electrochemical Cell

The Electrochemical Cell drawing can be seen on the left side of the Figure 18. The support structure is formed by two rectangular shaped slides with the dimensions of a standard glass slide and some screws to attached both parts together. The cell is the round centered hole in the upper slide. All the pieces are made of non-conductive polymer and to prevent solution leakage it was inserted an oring with the same diameter of the cell between the slides.

An important design detail is the thickness of the upper part that must be as thin as possible to not limit the performance for small working distances between the microscope and the SERS-electrode which is a crucial parameter for SERS analysis. Other important design feature is the diameter of the cell that must be as small as possible to show the SERS-active areas of the electrode and at the same time using small sample volumes just to cover the entire electrode surface.

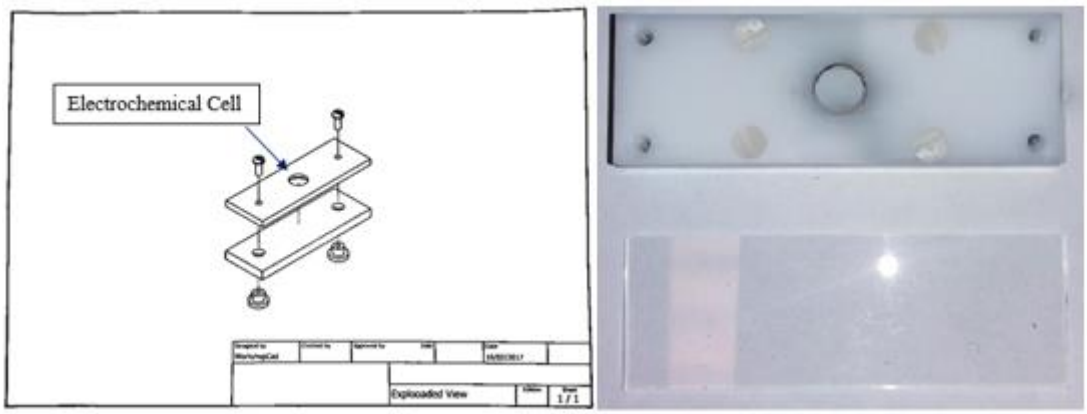

Figure 18- (left) Electrochemical Cell CAD drawing. (Right) Photo of the electrochemical Cell and a glass slide to compare the size.

3.2 Electrodes

To perform cyclic voltammetry measurements in the developed electrochemical cell Platinum and Carbon electrodes (from Zimmer and Peacock company) were used and they are shown in the Figure 19. To make the contact between the wires and the screen-printed electrodes silver paste was deposit and left dry during night. Then UV curable glue was deposit on top of the contacts to provide a stronger support and help isolate one contact from each other.

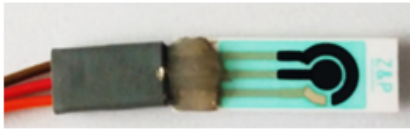

Figure 19 – Screen printed electrode, CE and WE are made of carbon and the reference electrode is Ag/AgCl.

3.3 Comparison between the Portable and a Commercial Potentiostat

To evaluate the performance of the Portable Potentiostat, Cyclic Voltammetry was performed. The standard reversible Ferricyanide-Ferrocyanide redox couple was used.

The comparison between the portable and a commercial potentiostat (Ana Pot from Zimmer and Peacock company) is shown in the Figure 20. It is possible to see the oxidation and reduction peaks occurring at the same potentials in both potentiostats. The same peak current is visualized in both cyclic voltammograms but there is a constant offset of the current measured between the cyclic voltammograms. This offset can be explained by a difference of the nominal resistance value from the 1 kΩ resistor where 3.3 V are added in the TIA. In the code 3.3 V are assumed to be added but by a slight change is the resistor values the offset value added can be different than 3.3 V.

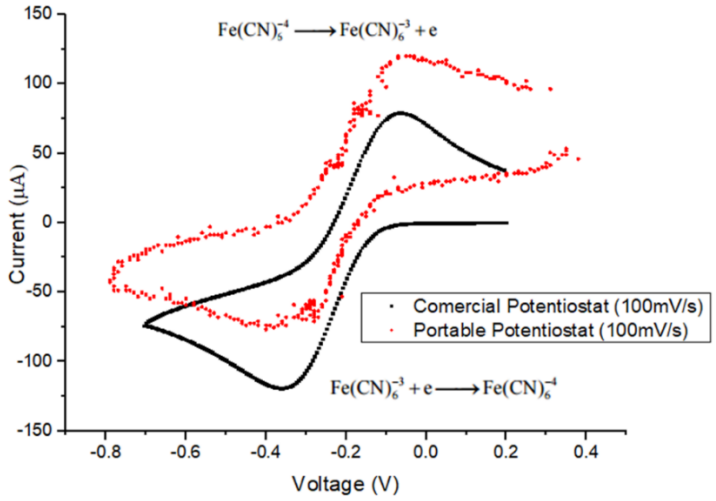

Figure 20 - Cyclic Voltammetry of 10mM of K3[Fe(CN)6] in 0.1M of NaCl for comparison of the portable and a commercial potentiostat. Scan rate of 100 mV/s.

3.4 Diffusion Coefficient Determination

To show the portable potentiostat capabilities cyclic voltammograms were also performed at different scan rates and by doing this the diffusion coefficient of potassium ferricyanide was calculated in a solution containing a known concentration of the salt using the Randles-Sevcik equation at 25 °C:

$$i_p = 2.69\times10^5\times n^{\frac{2}{3}}\times A\times D^{\frac{1}{2}}\times C_0\times v^{\frac{1}{2}} \quad (9)$$

The n is number of electrons transferred, the A is the working electrode area in cm^2, D is diffusion coefficient in cm^2/s, C_0 is concentration in mol/cm^3 and v is the scan rate in V/s.

The Carbon working electrode with a diameter of 4 mm. The electrochemical cell was filled with 5 mM potassium ferricyanide (from Sigma Aldrich) in 0.1 M NaCl (from Breckland Scientific Supplies Ltd) solution. The potential was swapped between 0.35 V and −0.85 V with scan rates of 0.8, 0.11, 0.14, 0.25, and 0.35 $V.s^{-1}$. The recorded data can be seen in Figure 21.

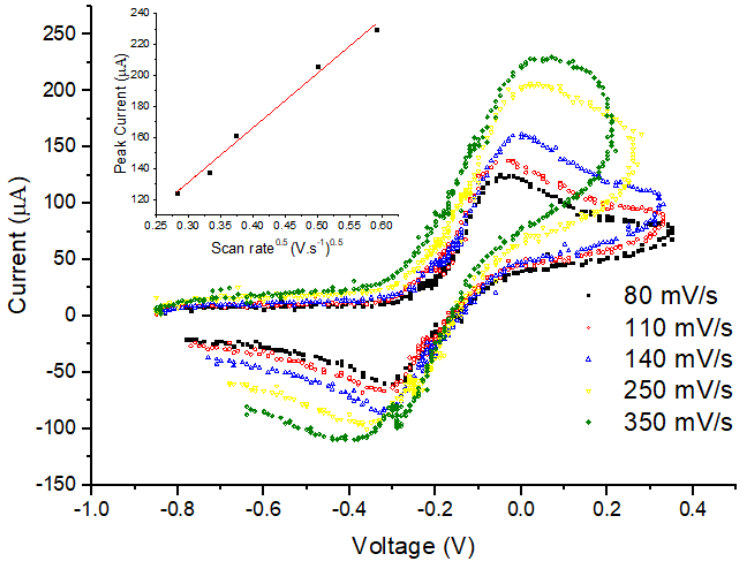

Figure 21 - Cyclic Voltammetry of 5mM of K3[Fe(CN)6] in 0.1M of NaCl at different scan rates. (Inset) Linear fit of the anodic peak currents against the square root of the scan rate.

As expected, Figure 21 shows an increase in the recorded electrochemical current with an increase in the scan rate. The inset shows the plot of the anodic peak current vs the square root of the scan rate. As expected, the plot is linear with a R^2 of 0.9993. From the calculated slope of the linear fit, using the Randles-Sevcik equation, the diffusion coefficient of potassium ferricyanide is calculated to be 4.3×10^{-6} $cm^2.s^{-1}$ which is in good agreement with the value in the literature.[14] [15] The difference between the values can be caused by the previous calibration of the scan rates before CV's were performed.

4 Experimental EC-SERS setup

The Figure 22 displays the experimental Setup for in situ EC-SERS. It includes the laser source to excite the SERS of samples, a Raman Microscope to disperse and detect the Raman signal, a computer to control the Raman instrument for data acquisition and manipulation, a potentiostat to control the potential and measure the current at the working electrode and a EC-SERS cell to carry out the reaction.

In this present work, the potentiostat used was the developed portable Potentiostat as shown in the picture which is connect to a computer, through a USB cable, to apply the desired potential and data acquisition. The Raman microscope used was the Horiba Labram Evolution HR.

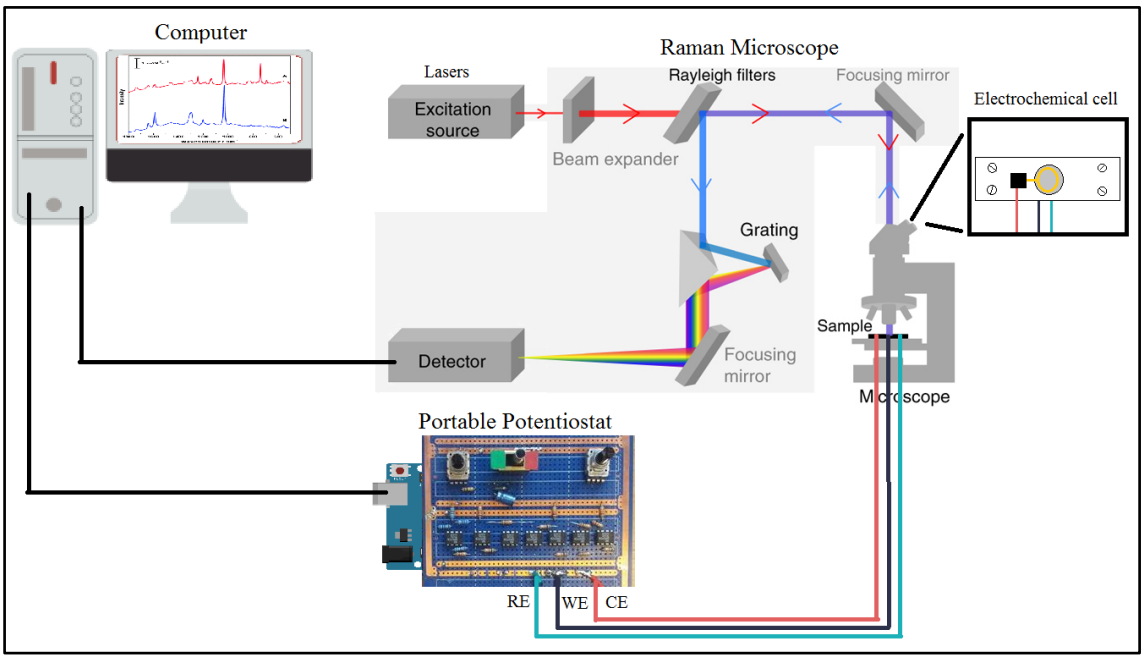

Figure 22 -Block Diagram of the experimental Setup for spectroelectrochemical SERS measurements.

4.1 EC-SERS cell

To perform electrochemical-SERS measurements the EC cell used before was modified. A slot was made on the side of the cell to fit the silver wire with 99.99% of purity from ABCR GmbH company (pseudo reference electrode). A ring-shaped gold wire 99,95% of purity from Alfa Aesar (counter electrode) was fixed on the top using an epoxy curable glue. SERS-active working electrode was introduced in between bottom and the top parts with the active area centered in the cell. This is all shown in the Figure 23.

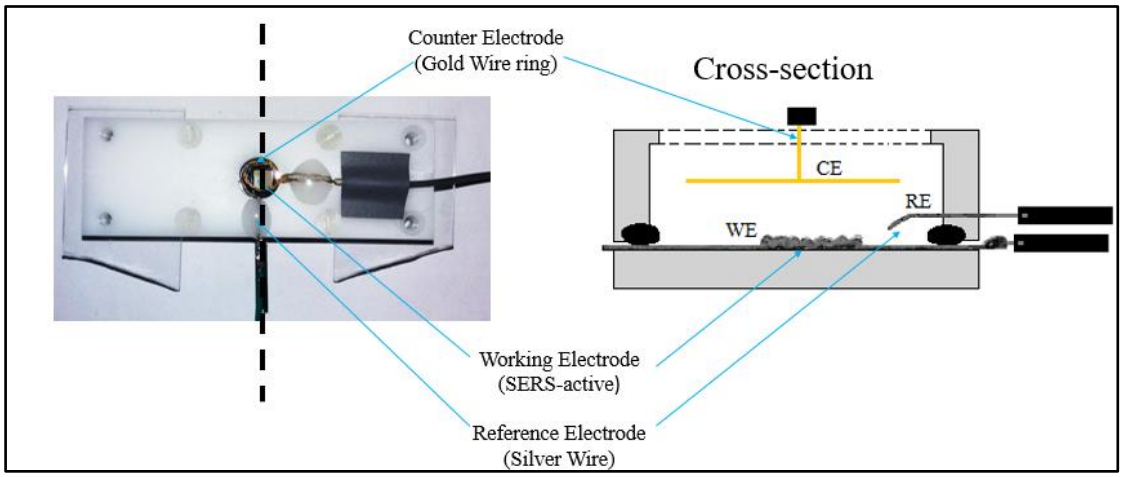

Figure 23 – Electrochemical cell with all electrodes assembled and its 90º rotated cross-section.

4.2 SERS-Active Working Electrode

The SERS-Active electrodes used are commercially available by the company ATOID™. The following description of the SERS substrates was provided by the company.

A stochastic nanostructure is formed on the surface of a soda-lime glass substrate by using a femtosecond laser pulses, depicted in the amplified image of the Figure 24. Then the substrates are washed in an ultrasonic bath and coated in a vacuum chamber using magnetron sputtering. Gold and Silver coated eletrodes were used.

Conductive Silver paste was used to make the contact of SERS eletrodes for use them as WE in the EC-SERS Cell, shown in the Figure 24.

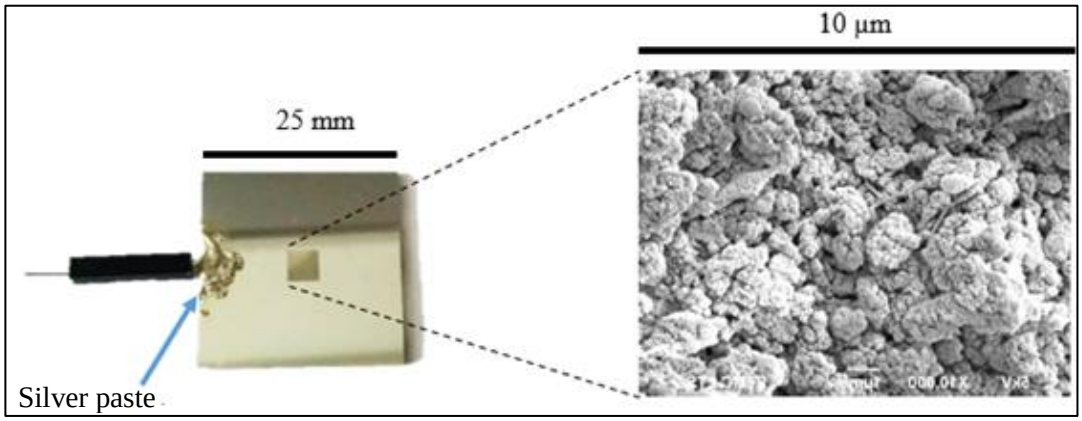

Figure 24 – SERS-active silver electrode and its 10,000 x magnified SEM image.

5 Results and discussion

5.1 SERS analysis of Rhodamine 6G (R6G)

R6G was used as the model analyte due to its large cross-section and strong SERS signal and also, EC-SERS measurements of R6G have not been done before. The strong visible absorption of R6G in aqueous solution has a maximum around 530 nm.[14] When R6G is excited with visible light at 532 nm, leads to larger enhancements due to a combination of the SERS effect that originates from surface plasmon excitation, and molecular resonance Raman effect.

However, it can generate high fluorescence yield which would prevent the observation of the Raman spectrum, [11] [16] thus the excitation laser wavelength used in this project was 633 nm.

To prove that the electrodes were SERS-active, 1 µM and 100 µM aqueous solutions of R6G were prepared and dropped onto the Silver SERS substrates and left dry before the Raman measurement. Doing the same procedure, 1 mM aqueous solutions of R6G was preapred and dropped on a SERS-inactive substrate (glass slide). The results are depicted in the Figure 25.

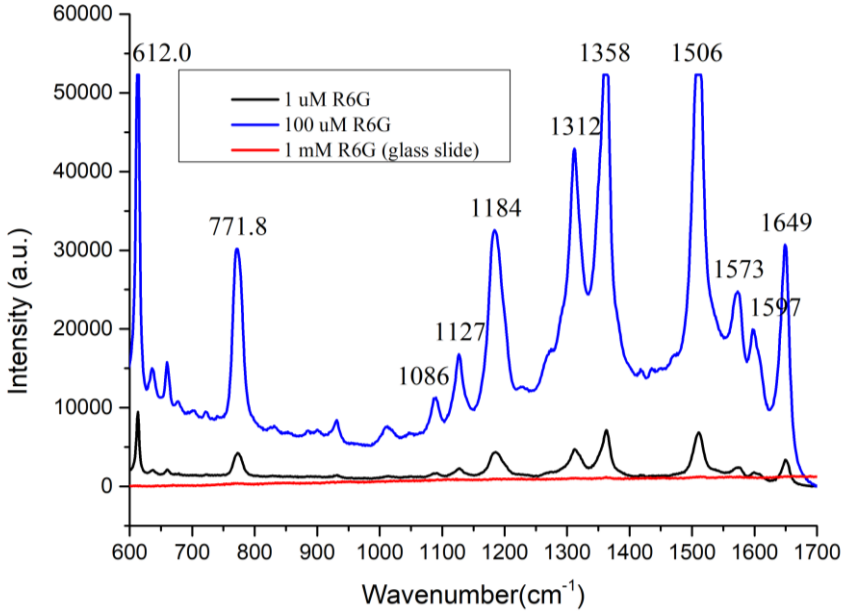

Figure 25 – SERS spectra of Rhodamine 6 G at different concentrations: 100 µM (Blue) and 1 µM (black) on silver coated SERS substrate. Normal Raman spectra collected for 1 mM of R6G on a glass slide (Red). All spectra were recorded using 10x magnification, laser ex.λ= 633nm with the power of 14 mW and acquisition time of 5 s. All baselines were subtracted.

As can be observed in the Figure 25, both of 1 and 100 µM aqueous solutions of R6G shows identical spectra with the expected increase of the intensities of the vibrational bands due to the increase of the concentration. It is also possible to visualize that even for a higher concentration, the vibrational peaks in the spectrum of 1 mM of R6G are hard to identify. This clearly pictures the SERS effect of the substrate on the analyte.

To identify the peaks of the Raman spectrum of 1 mM R6G aqueous solution a smooth averaging filter was applied and the baseline was subtracted increasing this way the signal to noise ratio as shown in the Figure 26.

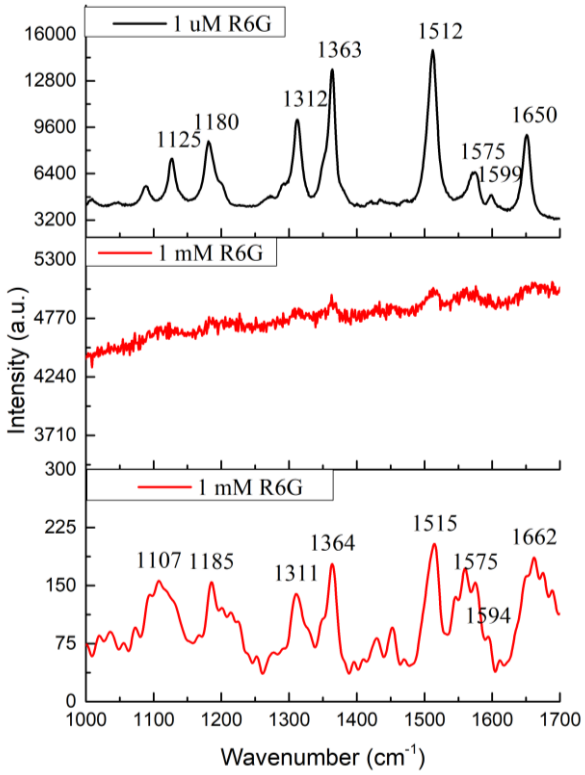

Figure 26 - SERS spectra of Rhodamine 6 G on silver SERS substrate for 1 µM (top) and Normal Raman spectra collected for 1 mM of R6G on a glass slide (center). Same Normal Raman spectra after applying averaging filter and subtract baseline (bottom).

From Figure 26, it is clear to see that even for a very weak signal it is possible to identify the major peaks in the Raman spectrum of 1 mM of R6G after increasing the signal to noise ratio. The areas of the vibrational bands around 1363 cm^{-1} and 1512 cm^{-1} of 1 µM solution of R6G SERS spectra were used to calculate the average EF value and it was approximately 7×10^5.

In both Raman and SERS spectra, the two main vibrational bands correspond to the aromatic C-C stretching modes around 1363 and 1512 cm^{-1}. The assignments of the vibrational bands are shown in Table 3 [11]. The difference between some peaks of the Raman and the SERS shown in the Table 3 are attributed to the small signal to noise ratio at their region of the spectrum.

Table 3 - Vibrational bands assignments for R6G.

Experimentally observed bands (cm^{-1})		**Assignments**
Raman	**SERS**	
1107	1125	in plane C-H bending
1185	1180	xanthene ring deformations, C-H bend, N-H bend
1311	1312	In plane xanthene ring breathing, N-H bending, CH2 waggling
1364	1363	Xanthene ring stretching, in plane C-H bending
1515	1512	Aromatic C-C stretching, xanthene ring stretching, C-N stretching, C-H bending, N-H bending
1575	1575	Xanthene ring stretching, in plane N-H bending
1594	1599	
1662	1650	Xanthene ring stretching, in plane C-H bending

5.2 EC-SERS study of Rhodamine 6G

In the present work, Electrochemical-SERS measurements of R6G were performed. The measurements were made by dropping 100 µL of 50 µM aqueous solution of R6G into the EC-SERS cell, then the cell was placed under the microscope objective and the Potential was scan from positive to negative potentials in respect to the reference electrode. In each potential step the SERS spectra of R6G was recorded. The time of each step was approximately 30 s. The results are show in the Figure 28.

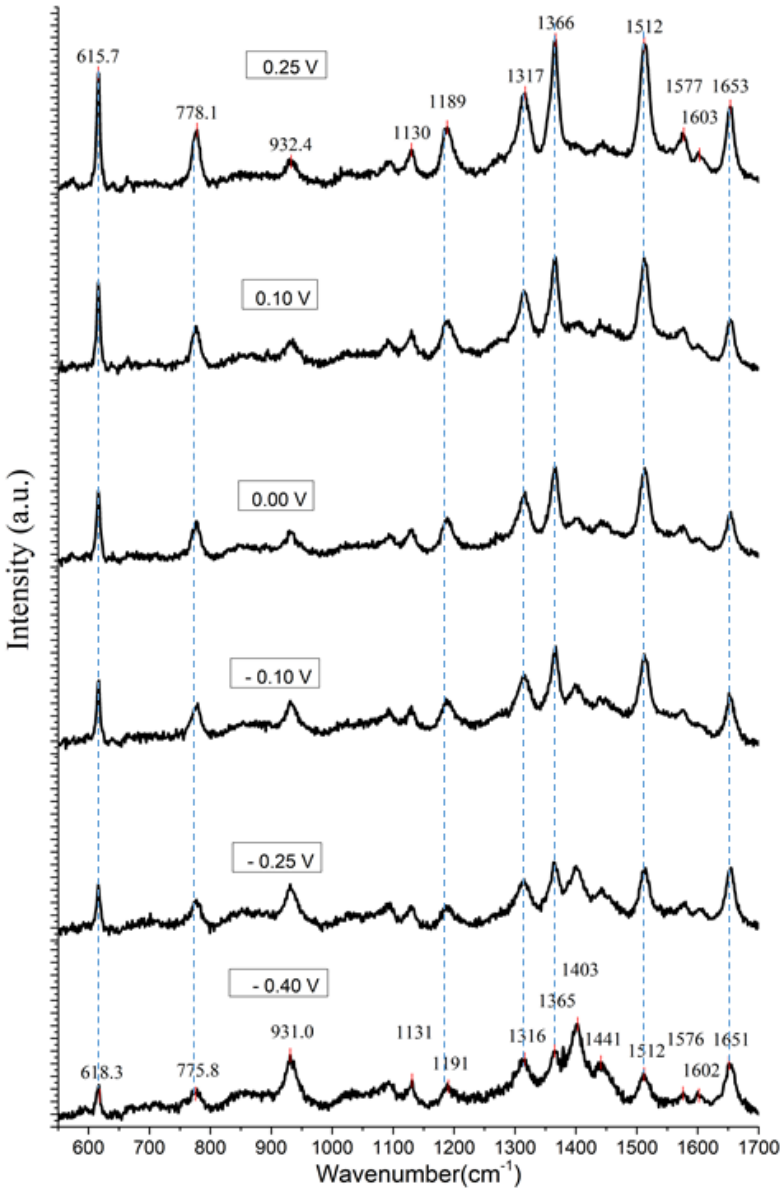

Figure 27 – SERS spectra of 50 µM aqueous solution of R6G on Silver Substrate under different Potentials. The scan was made from positive to negative potentials. All spectra were recorded using 10x magnification laser ex.λ= 633nm with the power of 14 mW and acquisition time of 5 s. All spectra were baseline corrected.

In the Figure 27**,** it is shown the spectra of R6G recorded at different potentials. For positive potentials, the spectra are identical to the off-resonance Raman spectrum obtain in [13] using the excitation wavelength of 1064 nm. From the vibrational peaks assignments in the Table 3 it is possible to visualize that most of them are related to xanthene ring deformations, breathing and stretching modes

which would explain a lay down configuration, where the delocalized π orbitals of the Xanthene are closer to the electrode surface.

And as the potential was change towards 0 V the spectra keep similar showing only a decrease in the intensity of the major vibrational peaks.

As the potential was moved towards negative potentials most of the vibrational bands of Rhodamine 6G keep decreasing their intensity except the two new vibrational peaks recorded at 1403 cm^{-1} 1441 cm^{-1} which increase the intensity instead and this can indicate the presence of a SERS-CT processes.

The CT mechanism can be explained by the resonant Raman mechanism in which charge-transfer excitations (either from the metal to the adsorbed molecule, or vice versa) occur at the energy of incident laser frequency. [17]

Among the peaks of the anomalous R6G SERS spectrum recorded at -0.4V, the ones recorded at 1403 cm^{-1} and 1441 cm^{-1}, assigned by Watanabe et Al. [13] to the vibrational modes ν_{126} and ν_{129}, respectively, are mainly localized in the phenyl region.

With an excitation frequency at 633 nm, adsorbates such as R6G having a narrow HOMO-LUMO band gap are electronically excited from the lower occupied orbitals to a Fermi level of silver surfaces, or from the Fermi level to higher virtual orbitals.

In the R6G molecule, occupied orbitals (ϕ116 and ϕ117) and a virtual orbital (ϕ120) calculated in [13] are the candidates for the CT electronic excitations in comparison with their energy differences from the increased Metal Fermi level and the excitation frequency. The calculated electron density distribution of the occupied orbitals (ϕ116 and ϕ117) is localized in the xanthene ring, and that of the virtual orbital (ϕ120) is centralized in the phenyl ring.

As the silver atoms of the electrode interact with the virtual orbital (ϕ120) at the phenyl ring of the R6G molecules, the bands (ν_{126} and ν_{129}) due to symmetric deforming motions of the phenyl ring could be very highly enhanced in their SERS intensities.

The EC-SERS measurements of R6G were also performed on gold substrate however a bigger potential range was used, the results are show in the Figure 28.

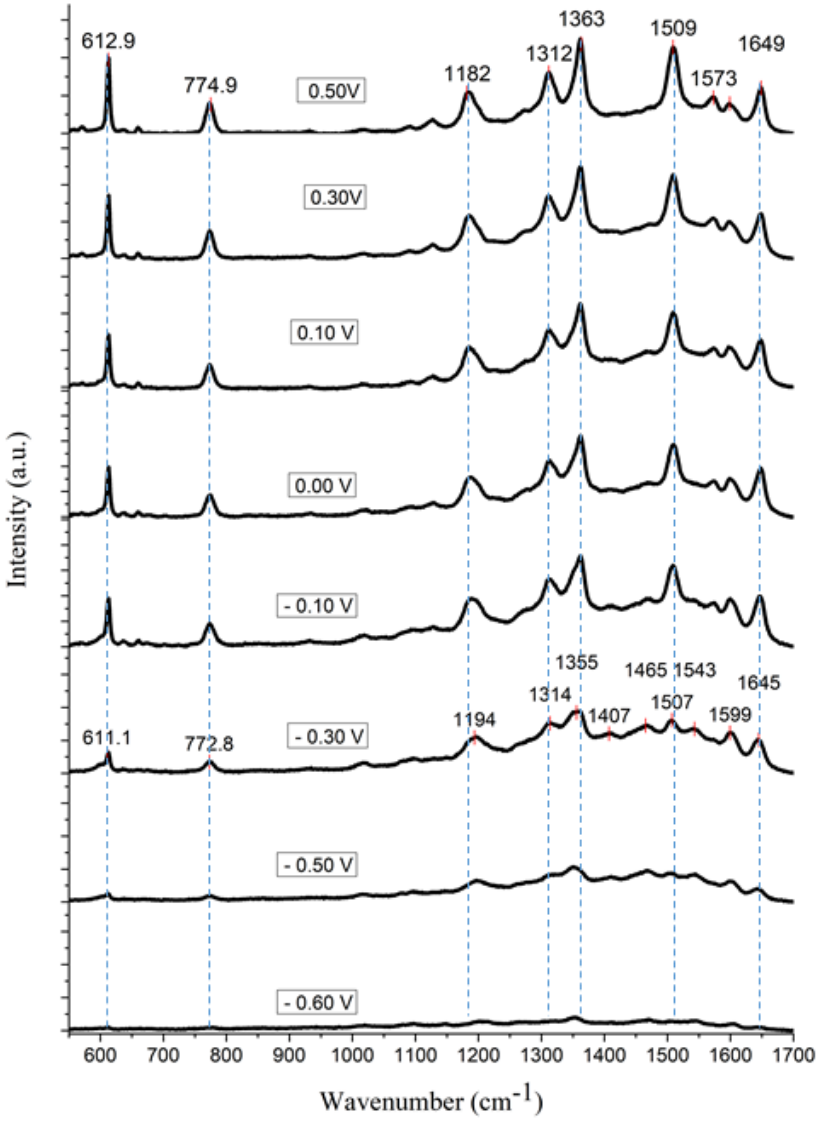

Figure 28 - SERS spectra of 50 µM aqueous solution of R6G on Gold Substrate under different Potentials. All spectra were recorded using 10x magnification laser ex.λ= 633nm with the power of 14 mW and acquisition time of 5 s. All spectra were baseline corrected.

For gold substrates, an identical behavior of the EC-SERS spectra was obtained, i.e., for more positive potentials the major peaks of R6G, mostly assigned to the Xanthene ring motions, are more intense which can be explained, by the surface selection rules, that it is due to the proximity of the carrier of the Xanthene ring to the metal surface. [18]

As the potential is changed from positive to negative values, again, all the R6G major peaks decrease in intensity except the two vibrational modes 1407 cm^{-1} and 1465 cm^{-1} that increase in intensity. These two vibrational peaks are quite broad and they can arise from the contribution of several vibrational modes, however some contributions can be assigned to the vibrational modes ν_{126} and ν_{137}, respectively, which again are mainly localized in the phenyl region.

Despite these vibrational modes being different from those obtained in Silver Substrate, this can again indicate the presence of a SERS-CT processes and the change in the vibrational energies can be attributed to the interaction between the molecule and the metal.

By using a bigger potential range, in the Figure 28, it is possible to visualize that the R6G spectrum is almost unrecognizable for negative potentials of -0.6 V. This significantly decrease of the SERS spectrum of R6G can be explained by the excitation energy that does not fall in an ideal resonance condition. Therefore, the contribution of vibrational states to the SERS signal will decrease. [5]

5.3 Concentration of R6G under constant potential

To further understand the behaviour of SERS signal under an applied potential, time dependent SERS measurements were performed under a constant applied potential.

The Figure 29 shows the variation in SERS spectra of R6G at different times applying a constant potential at the SERS-active silver electrode. The potential used for this experiment was 0.25V since for positive voltages the SERS spectrum of R6G shows the highest intensities for most of the vibrational peaks.

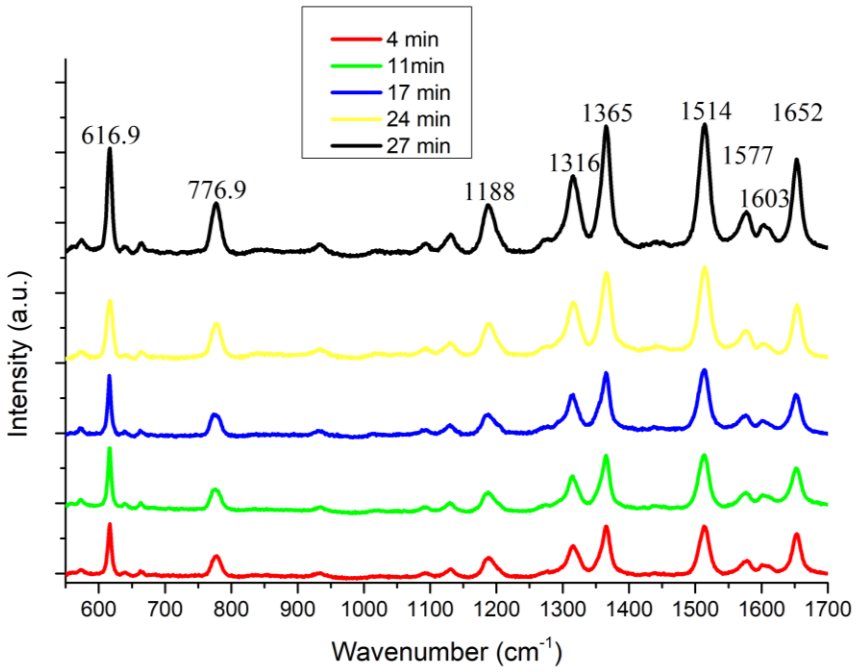

Figure 29 – SERS spectra of 50 µM aqueous solution of R6G on Silver with applied potential of 0.25V over different times. All spectra were recorded using 10x magnification, laser ex.λ= 633nm with the power of 14 mW of and acquisition time of 5 s. All spectra were baseline corrected.

Figure 29 clearly demonstrates the substantial enhancement of the SERS peaks for 50 µM aqueous solution of R6G under a constant electric field as time passed by. Also the major peaks increased approximately at same ratios which it not in agreement with the results recorded by M. Park et Al. [19], where they performed the same concentration measurements for R6G but different peaks have different growths. This difference can be attributed to the initial concentration which can play a role in the molecular orientation. Although it is not clearly understood.

The Figure 30 demonstrates the SERS peak intensity recorded at 1512 cm^{-1} applying the previous constant electric fields vs no electric field applied. The experimental results indicate that for the first 28 minutes of constant electric filed applied, the peak intensity increase at different rates showing a higher intensity growth after 16 minutes and this result are a lot in agreement with experimental results achieved before in [19]. Although PBS solution was not used as electrolyte the Rhodamine 6G provided by sigma Aldrich has chloride ions and its believed that in solution they are

responsible for the electrolytic conduction. The SERS peak oscillations without any electric field applied can be explained by the adsorption and desorption of the analyte from the surface.

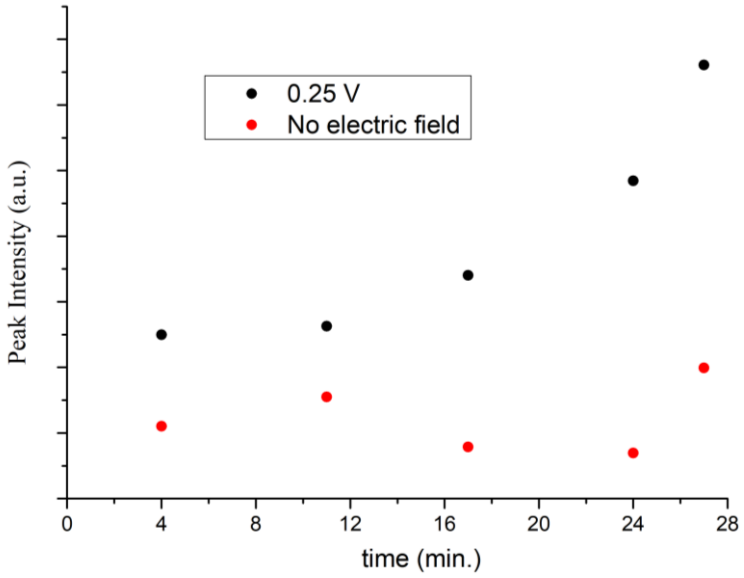

Figure 30 – 1512 cm^{-1} peak intensity over time with and without applied potential.

The concentration study performed by M. Park et Al. [20] shows a maximum SERS signal enhancement for all target concentrations after 30 minutes of injection time, however in the present experiment a higher initial concentration was used and the SERS signal began to saturate after 28 minutes of the experiment. Despite of this the same maximum concentration time would be expected.

6 Conclusions and perspectives

The main objective of this work was to perform an Electrochemical-SERS study of R6G using Silver and Gold SERS-active Electrodes. For that a portable microcontroller based Potentiostat was developed to fit in the Raman microscope to perform potential scan at the SERS working electrode.

Here it was demonstrated a portable Potentiostat prototype that can perform electrochemical measurements, such has cyclic voltammetry or potential step voltammetry by changing the signal applied. Using a simple potentiometer, the user can adjust the voltage range. Also, the scan rate of cyclic voltammetry measurements can be tuned. The data acquisition through the USB cable can be displayed in real time using the open source Processing as a Serial terminal program which can also save the data in text file format for further analysis.

Although the potentiostat worked fine it can be improved using op-amps with single supply to get rid of the 9V power supply batteries achieving this way more portability, i.e., being totally USB power supplied.

It was also demonstrated EC-SERS cell prototype that fits in the Raman microscope stage showing a good stability for measurements. A few improvements can also be done to have a better performance, like the walls of the cell can be tilted to hold smaller sample volumes which can be crucial for very low analyte solution volumes and a slot can also be done to fit the Counter electrode in a more stable position.

The experimental evidence has shown that R6G has changes in SERS spectra and they are briefly discussed in relation to the enhanced vibrational modes and the corresponding electronic excitations. These enhancement mechanisms are presumed to be a result of mainly the conventional CT mechanism of SERS. They result from the combination of the increase of surface charge through the potential applied at the metal electrode and the excitation wavelength.

The results provide insights into the SERS spectrum of excited states of R6G at wavelength that are out of maximum absorption. Thus, by this technique it is possible to access the excited states of molecules which otherwise using solely higher excitation energies would be difficult to access due to strong fluorescence. It is found that theoretical calculations of R6G are in good agreement with experimental results, where CT states are mainly localized in the phenyl ring, even though solvent effects are not being take in account.

However, there are some very important issues which remain unanswered, unclear and even somewhat ambiguous to the attribution of the signal. A reliable observation of the shift in the potential with the excitation wavelength to demonstrate the CT process in an electrochemical environment at a very low laser power density is hard to achieved. All experimental conditions must be optimized to reject any kind error introduced by the setup.

Microfluidic devices offer unique advantages for EC-SERS application. The use of small sample volumes confined in very small channels along with the possibility for integration of the electrodes in the microfluidics chips will allow to obtain much reliable EC-SERS results. The key challenges are on the reliable preparation and stable SERS-active substrates inside the microfluidic channels.

References

[1] Z. Tian, B. Ren, and D. Wu, "Surface-Enhanced Raman Scattering : From Noble to Transition Metals and from Rough," vol. 106, no. 37, 2002.

[2] T. Vo-Dinh, "Surface-enhanced Raman spectroscopy using metallic nanostructures," *TrAC - Trends Anal. Chem.*, vol. 17, no. 8–9, pp. 557–582, 1998.

[3] N. Valley, N. Greeneltch, R. P. Van Duyne, and G. C. Schatz, "A look at the origin and magnitude of the chemical contribution to the enhancement mechanism of surface-enhanced Raman spectroscopy (SERS): Theory and experiment," *J. Phys. Chem. Lett.*, vol. 4, no. 16, pp. 2599–2604, 2013.

[4] F. Avila, C. Ruano, I. Lopez-Tocon, J. F. Arenas, J. Soto, and J. C. Otero, "How the electrode potential controls the selection rules of the charge transfer mechanism of SERS," *Chem. Commun.*, vol. 47, no. 14, p. 4213, 2011.

[5] D. Wu, J. Li, B. Ren, and Z. Tian, "Electrochemical surface-enhanced Raman spectroscopy of nanostructures," pp. 1025–1041, 2008.

[6] Z.-Q. Tian *et al.*, "Surface-enhanced Raman scattering from transition metals with special surface morphology and nanoparticle shape," *Faraday Discuss.*, vol. 132, pp. 159–170, 2006.

[7] U. Kreibig and M. Vollmer, "Optical Properties of Metal Clusters," *J. Am. Chem. Soc.*, vol. 118, no. 25, pp. 6098–6098, 1995.

[8] D. Y. Wu, M. Hayashi, S. H. Lin, and Z. Q. Tian, "Theoretical differential Raman scattering cross-sections of totally-symmetric vibrational modes of free pyridine and pyridine-metal cluster complexes," *Spectrochim. Acta - Part A Mol. Biomol. Spectrosc.*, vol. 60, no. 1–2, pp. 137–146, 2004.

[9] C. Novo, A. M. Funston, A. K. Gooding, and P. Mulvaney, "Electrochemical Charging of Single Gold Nanorods Carolina," pp. 14664–14666, 2009.

[10] A. H. Ali and C. A. Foss, "Electrochemically Induced Shifts in the Plasmon Resonance Bands of Nanoscopic Gold Particles Adsorbed on Transparent Electrodes," *J. Electrochem. Soc.*, vol. 146, no. 2, pp. 628–636, 1999.

[11] L. Jensen and G. C. Schatz, "Resonance Raman scattering of rhodamine 6G as calculated using time-dependent density functional theory.," *J. Phys. Chem. A*, vol. 110, no. 18, pp. 5973–5977, 2006.

[12] J. Guthmuller and B. Champagne, "Resonance Raman scattering of rhodamine 6G as calculated by time-dependent density functional theory: Vibronic and solvent effects," *J. Phys. Chem. A*, vol. 112, no. 14, pp. 3215–3223, 2008.

[13] H. Watanabe, N. Hayazawa, Y. Inouye, S. Kawata, and T. R. Spectroscopy, "DFT Vibrational Calculations of Rhodamine 6G Adsorbed on Silver : Analysis of Tip-Enhanced Raman Spectroscopy DFT Vibrational Calculations of Rhodamine 6G Adsorbed on Silver : Analysis of," *J. Phys. Chem. B*, vol. 11, no. 109, pp. 5012–5020, 2005.

[14] B. Aremo, M. Oyebamiji Adeoye, I. B. Obioh, and O. A. Adeboye, "A Simplified Microcontroller Based Potentiostat for Low-Resource Applications," *Open J. Met.*, vol. 5, no. 4, pp. 37–46, 2015.

[15] G. N. Meloni, "Building a microcontroller based potentiostat: A inexpensive and versatile platform for teaching electrochemistry and instrumentation," *J. Chem. Educ.*, vol. 93, no. 7, pp. 1320–1322, 2016.

[16] W. E. Smith, "Practical understanding and use of surface enhanced Raman scattering/surface enhanced resonance Raman scattering in chemical and biological analysis," *Chem. Soc. Rev.*, vol. 37, no. 5, p. 955, 2008.

[17] A. Campion, P. Kambhampati, A. Campion, and C. Harris, "Surface-Enhanced Raman Scattering," vol. 103, pp. 241–250, 2006.

[18] M. Moskovits and J. S. Suh, "Surface selection rules for surface-enhanced Raman spectroscopy: calculations and application to the surface-enhanced Raman spectrum of phthalazine on silver," *J. Phys. Chem.*, vol. 88, no. 2, pp. 5526–5530, 1984.

[19] Y. S. Huh, A. J. Chung, B. Cordovez, and D. Erickson, "Enhanced on-chip SERS based biomolecular detection using electrokinetically active microwells †," pp. 433–439, 2009.

[20] M. Park, Y. Oh, S. Park, and S. Yang, "Electrokinetic Preconcentration of Small Molecules Within Volumetric Electromagnetic Hotspots in Surface Enhanced Raman Scattering," pp. 2487–2492, 2015.

7 Attachments

Processing code

```
import processing.serial.*;
Serial mySerial;
PrintWriter output;
void setup() {
  mySerial = new Serial( this, "COM3", 9600 );//choose the USB port for serial
imput
  output = createWriter( "data.txt" );//creates a text file in the same
directory of the Sketch
  size(600, 400); // set the window size:
  background(255);// set initial background
  strokeWeight(2);  // Default
  line(40, 360, 580, 360);//x axis
  line(40, 40, 40, 360);//y axis
  line(40, 360, 40, 365);//x line lower limit
  line(580, 360, 580, 365);//x line upper limit
  line(302, 360, 302, 365);//0 line
  textSize(15);
  fill(0, 102, 153);
  text("Voltage (V)", 285,390);//X axis label
  fill(0, 102, 153);
  text("-1.2", 30, 380);
  fill(0, 102, 153);
  text("0", 300, 380);
  fill(0, 102, 153);
  text("1.2", 575, 380);
  fill(0, 102, 153);
  rotate(-PI/2);
  text("Current", -235, 30); // y axis label

}
//function that reads the serial values as strings and converts them in num
bers then it plots them and prints them on text file
void draw() {
  if (mySerial.available() > 0 ) {
    String value = mySerial.readStringUntil('\n');
    if ( value != null ) {
      println(value);
      int p1 = value.indexOf(" ");
      int l=p1-1;
      String ss = value.substring(0, l+1);
      String ss1 = value.substring(p1);
      float voltage = float(ss);// convert to a number.
      float current = float(ss1);// convert to a number.
      println(voltage + " " + current);
      output.println(voltage + " " + current);
      float volt = map(voltage, -1.2, 1.2, 40, 580);//map to the screen width
      float curr = map(current, -1, 1, 360, 40); //map to the screen height
      ellipse(volt, curr, 3, 3);
    }
  }
}
//funtion to close the plot and save the file when any key of the keyboard
is pressed
void keyPressed() {
```

```
    output.flush();  // Writes the remaining data to the file
    output.close();  // Finishes the file
    exit();  // Stops the program
}
```